Studies of radiation absorption on flame speed and flammability limit of CO2 diluted methane flames at elevated pressures

Chen, Zheng; Qin, Xiao; Xu, Bo; Ju, Yinguang; Liu, Fengshan

Publisher's version / Version de l'éditeur:
https://doi.org/10.1016/j.proci.2006.07.202
Proceedings of the Combustion Institute, 31, January 2, pp. 2693-2700, 2007

Available online at www.sciencedirect.com
ScienceDirect
Proceedings of the Combustion Institute 31 (2007) 2693–2700
Proceedings of the Combustion Institute
www.elsevier.com/locate/proci

Studies of radiation absorption on flame speed and flammability limit of CO_2 diluted methane flames at elevated pressures

Zheng Chen [a,*], Xiao Qin [a], Bo Xu [a], Yiguang Ju [a], Fengshan Liu [b]

[a] Department of Mechanical and Aerospace Engineering, Princeton University, Princeton, NJ 08544, USA
[b] Combustion Research Group, National Research Council Canada, 1200 Montreal Road, Building M-9, Ottawa, Ont., Canada K1A 0R6

Abstract

The effects of spectral radiation absorption on the flame speed at normal and elevated pressures were experimentally and numerically investigated using the CO_2 diluted outwardly propagating CH_4–O_2–He flames. Experimentally, the laminar burning velocities of CH_4–O_2–He–CO_2 mixtures at both normal and elevated pressures (up to 5 atm) were measured by using a pressure-release type spherical bomb. The results showed that radiation absorption with CO_2 addition increases the flame speed and extends the flammability limit. In addition, it was also shown that the increase of pressure augments the effect of radiation absorption. Computationally, a fitted statistical narrow-band correlated-*k* (FSNB-CK) model was developed and validated for accurate radiation prediction in spherical geometry. This new radiation scheme was integrated to the compressible flow solver developed to simulate outwardly propagating spherical flames. The comparison between experiment and computation showed a very good agreement. The results showed that the flame geometry have a significant impact on radiation absorption and that the one-dimensional planar radiation model was not valid for the computation of the flame speed of a spherical flame. An effective Boltzmann number is extracted from numerical simulation. Furthermore, the FSNB-CK model was compared with the grey band SNB model. It was shown that the grey band SNB model over-predicts the radiation absorption. It is concluded that quantitative prediction of flame speed and flammability limit of CO_2 diluted flame requires accurate spectral dependent radiation model.

Keywords: Spectral dependent radiation; Burning velocity; Flammability limit; CO_2 addition

1. Introduction

Thermal radiation receives a renewed interest because it is a dominant transport mechanism in space, urban fires, and ultra lean high pressure combustion. The strong spectral radiation absorption of CO_2 and the appearance of large amount of CO_2 in the exhausted gas recirculation and CO_2 fire suppressant raise the following question: what is the role of CO_2 radiation in flame speed and flammability limit? This concern becomes more serious when the ambient pressure increases. Recently, it has become clear that spectral radiation is the dominant loss

* Corresponding author. Fax: +1 609 258 6233.
E-mail address: zhengc@princeton.edu (Z. Chen).

1540-7489/$ - see front matter © 2006 The Combustion Institute. Published by Elsevier Inc. All rights reserved.
doi:10.1016/j.proci.2006.07.202

mechanism for flammability limit [1–5] and it leads to radiation extinction [6–9], flame bifurcations [10–12] and radiation induced instability [13]. Therefore, the effect of radiation heat loss on near limit flames has been extensively studied [1–5,14–17]. However, CO_2 is not only a radiation emitter but also an absorber.

The effect of radiation absorption on flame speed was first analyzed by Joulin and Deshaies [18] using a gray gas model. It was shown that there is no flammability limit when radiation absorption is considered. The gray model was also used to study flame ball dynamics [19]. However, CO_2 radiation is not gray. Rather, it is spectral dependent and has temperature and pressure broadening. Ju and his coworkers [20,21] first used the non-gray statistical narrow band (SNB) model in studying the CO_2 diluted propagating flames and showed that a "fundamental" flammability limit exists because of the emission-absorption spectra difference between the reactants and products and band broadening. This model was later used in flame balls [22] and high pressure planar flames [23]. However, even the prediction was better than that of optically thin model [8,9], it still could not reproduce the experimental data [7]. Moreover, because of the limitation of computation time, radiation modeling [20] still used the gray assumption on each spectral line and was limited to one-dimensional (1D) planar flame geometry although many experimental data are from spherical flames. More importantly, experimental data of radiation absorption was not available to validate the modeling. Although Abbud-Madrid and Roney [24] tried to measure the radiation absorption effect using a particle laden flame, the radiation effect is not yet confirmed because of the large heat capacity of particles. Therefore, it is particularly important to: (1) obtain experimental data of CO_2 spectral radiation absorption to validate radiation modeling; (2) develop accurate and efficient radiation model; and (3) understand the dependence of radiation absorption on pressure, flame scale, and flame geometry.

The goal of this study was to experimentally measure the effect of radiation absorption on flame speed at elevated pressures using the CO_2 diluted outwardly propagating CH_4–O_2–He flames and to develop a more accurate and efficient spectral radiation model for spherical flame modeling. First, the flame speed and flammability limit of the CO_2 diluted flames were measured. A new radiation model was then developed and validated using the measured data. Finally, the dependence of radiation absorption on pressure and flame scale was examined and the Boltzmann number for radiation absorption was computed.

2. Experimental method

The experimental measurements of flame speed were conducted in a dual-chambered, pressure-release type high pressure combustion facility at normal gravity [25]. Due to the effect of buoyancy, the maximum test pressure was limited to 5 atm. The combustible mixture was spark-ignited at the center of the inner chamber with minimum ignition energy so as to minimize ignition disturbances. The flame propagation sequence was imaged with Schlieren photography and a high-speed digital video camera (Photron Fastcam APX) with 4 μs shutter speed and a frame rate of 8000 fps was used. 1024 pixels were used for 5 cm width domain in horizontal direction. Data reduction was performed only for flame radii between 1.0 and 2.5 cm. The pressure increase is negligible because the volume of the chamber is approximately 100 times larger than the flame size at which flame speed was measured.

The stretched flame speed was first obtained from the flame history and then was linearly extrapolated to zero stretch rate to obtain the unstretched flame speed [25]. The estimated measurement uncertainty is ~5%. The reactant mixtures were prepared using the partial pressure method. Helium was introduced to adjust the mixture Lewis number (Le) to suppress the flame instability. Mixtures of $CH_4 - \{0.3O_2 + 0.2He + 0.5CO_2\}$, with $Le = 1.15$–1.20, were examined and all runs were performed in a quiescent environment at an initial temperature of 298 ± 3 K and initial pressures ranging from 1 to 5 atm. The results presented at each point were the average of three tests.

3. Fitted SNB-CK radiation model and numerical algorithm

For combustion gas radiation properties, a number of databases have been compiled based on line-by-line (LBL) [26,27], and narrow band [28,29] model, and global full-spectrum model [30,31]. The LBL is accurate at low temperatures, but requires excessive CPU time and is not suitable for high temperature combustion gases because the high temperature vibration-rotation absorption bands are not included. For global models, the weighted-sum-of-grey-gases (WSGG) model [30] and the full-spectrum correlated-k methods [31] were developed. These models have excellent computation efficiency but are less accurate than the band models and have difficulties treating non-gray boundaries. The statistical narrow-band (SNB) models [28] are favored. Recent CO_2 absorption experiment [32] showed that EM2C SNB model has an excellent accuracy up to 1300 K. In the SNB model for non-homogeneous mixtures, the ray tracing method [33] and

the Curtis–Godson approximation were widely used [33,34]. However, the ray tracing method is computationally inefficient, and the Curtis–Godson approximation is accurate only in the optically thick and thin limits.

Lacis et al. [35] developed a new category of the SNB based correlated-k method (SNBCK). By reordering the absorption coefficients in LBL into a monotonic k-distribution in a narrow spectral range, the model can produce exact results at a small computation cost [36]. For inhomogeneous media, it was shown that CK model gives much better results than the standard Curtis–Godson correlation. Furthermore, it allows the implementation of conventional discrete ordinate method (DOM) [37]. However, the inversion of CK model requires numerical iterations and sometimes convergence is not guaranteed. In addition, the SNB-CK model has not been considered in radiation modeling for spherical flames.

In this study, to resolve the convergence difficulty of SNB-CK in multi-component mixtures and to increase the computation efficiency, we developed a fitted SNB-CK model and extended it for radiation calculation of spherical flames. Hereafter, we call this model FSNB-CK.

In the SNB model, the gas transmissivity, τ_v, at wave number v over a light path L is given as [38]

$$\tau_v = \exp\left[-\pi b\left(\sqrt{1+4SL/\pi b}-1\right)/2\right] \tag{1}$$

where $b = 2\bar{\beta}_v/\pi$, $S = \bar{k}_v Xp$, and $\bar{\beta}_v = 2\pi\bar{\gamma}_v/\bar{\delta}_v$ are the SNB model parameters [28] for CO, CO_2 and H_2O. The bandwidth is $25\,cm^{-1}$ for wave numbers between 150 and $9300\,cm^{-1}$. By performing an inverse Laplace transformation, the distribution function of the absorption coefficient at each narrow band can be obtained as [35]

$$f(k) = 0.5k^{-3/2}(bS)^{1/2} \times \exp\left[0.25\pi b(2 - S/k - k/S)\right] \tag{2}$$

and the cumulative function of k-distribution

$$g(k) = \int_0^k f(k')\,dk' \tag{3}$$

can be given as

$$g(k) = \frac{1}{2}\left[1-\mathrm{erf}\left(\sqrt{\frac{\pi bS}{4k}}-\sqrt{\frac{\pi bk}{4S}}\right)\right] + \frac{1}{2}\left[1-\mathrm{erf}\left(\sqrt{\frac{\pi bS}{4k}}+\sqrt{\frac{\pi bk}{4S}}\right)\right]\exp(\pi b) \tag{4}$$

Using the cumulative distribution function, the average radiation intensity at each narrow band can be calculated using a Gauss type quadrature [36]

$$I_v = \sum_{i=1}^{N}\omega_i I_v[k_i(g_i)] \tag{5}$$

where N is the number of Gaussian quadrature points, ω_i the weight function, and g_i the Gaussian point. The estimation of $k_i(g_i)$ from Eq. (4) needs iterations and sometimes diverges for multi-component mixtures [35]. In order to resolve this problem, we rewrote Eq. (4) as

$$k_{ii}/S(b) = F_i(b), \quad i = 1,\ N \tag{6}$$

Here, $F_i(b)$ is a fitted function at all Gaussian points for CO, CO_2 and H_2O using the SNB data [28], respectively. Therefore, Eq. (4) is replaced by Eq. (6) using $3\times N$ fitted functions. Since a four-point Gaussian quadrature is accurate enough for Eq. (5), we only need 12 fitting functions. These fittings are straight forward and the maximum error between $B = 10^{-4}$ and 10^4 for k_i/S is less than 0.5%. For $b < 10^{-4}$ and $b > 10^4$, the optically thin and thick limits can be applied. The use of Eq. (6) and high accuracy of fitting completely remove the need of iteration for $k_i(g_i)$ from Eq. (4) and thus this technique avoids the problem of divergence.

For radiating gas mixtures, the approximate treatment of overlapping bands from optically thin and thick limits [35,36] is employed

$$S = S_{CO} + S_{CO_2} + S_{H_2O},\ S^2/b = S^2_{CO}/b_{CO} + S^2_{CO_2}/b_{CO_2} + S^2_{H_2O}/b_{H_2O} \tag{7}$$

The contribution from soot radiation at each narrow band can be added to the gas phase radiation. The spectral radiative transfer equation in spherical coordinates at each band in m direction is given as

$$\mu_m\frac{\partial I_{vm}}{\partial r} + \frac{2\mu_m I_{vm}}{r} + \frac{1}{r}\frac{\partial}{\partial\mu_m}[(1-\mu_m^2)I_{vm}] = -k_v I_{vm} - k_v I_{bv} \tag{8}$$

where $\mu_m = \cos(\theta_m)$, and m is the index from 1 to M of polar angle θ, and I_b the blackbody radiation intensity.

By using the following angular derivative,

$$\frac{\partial}{\partial\mu_m}[(1-\mu_m^2)I_{vm}] = \frac{\alpha_{m+1/2}I_{m+1/2} - \alpha_{m-1/2}I_{m-1/2}}{\omega_m}$$
$$\alpha_{m+1/2} - \alpha_{m-1/2} = -2\omega_m\mu_m, \quad \alpha_{1/2} = \alpha_{M+1/2} = 0 \tag{9}$$

and the central difference scheme for spatial and angular discretizations,

$$2I^C_{i+1/2,m} = I_{i,m} + I_{i+1,m} = I^C_{i+1/2,m+1/2} + I^C_{i+1/2,m-1/2} \tag{10}$$

the final discretized radiation transfer equation for $\mu_m < 0$ becomes

$$2|\mu_m|\frac{I^C_{v,i+1/2,m}-I_{v,i+1,m}}{r_{i+1}-r_i}+\frac{(\alpha_{m+1/2}+\alpha_{m-1/2})(I^C_{v,i+1/2,m+1/2}-I^C_{v,i+1/2,m})}{r_{i+1/2}\omega_m}=k_v(-I_{v,i+1/2,m}+I_{bv,i+1/2}) \tag{11}$$

The boundary conditions at r = 0 and $r = r_2$ are given as

$$I_m = I_{M+1-m} \text{ at } r=0; \quad I_m = \varepsilon_w I_{bw}(T_w)+(1-\varepsilon_w)\sum_{\mu_m>0} I_m w_m \mu_m/\pi \text{ at } r=R \tag{12}$$

The total volumetric heat source term of radiation is given as

$$\dot{q}_r = \sum_{j=1}^{N\text{-band}} \Delta v \sum_{n=1}^{N} \omega_n k_n \left(\sum_{m=1}^{M} I_{j,n,m} - 4\pi I_{bj}\right) \tag{13}$$

For spherical flame simulation, due to the pressure change and the pressure induced compression wave, we employed the unsteady compressible Navier–Stokes equations for multi-species reactive flow. The central difference scheme and the Euler scheme were employed for the diffusion and time integrations, respectively. The convective flux is calculated by the HLLC Riemann solver [39]. To numerically resolve the moving flame front, an adaptive mesh refinement algorithm was developed. The mesh addition and removal are based on the first and second order gradients of the temperature and major species distributions. Adaptive mesh of eight-level was used and the moving reaction zone was always fully covered by finest meshes of 30 μm in width. This adaptive algorithm is much more efficient than that used in the CHEMKIN package [40]. For methane oxidation, the GRI-MECH 3.0 mechanism [41] was used and the detailed transport and thermodynamic properties were predicted from the CHEMKIN database [40]. To initiate the computation, a hot spot with radius of 1.5 mm and temperature of 1800 K was set in the center initially to mimic the spark ignition in experiments. The same as experiments, the stretched flame speed was first obtained from the flame front (point of maximum heat release) history and then was linearly extrapolated to zero stretch rate to obtain the unstretched flame speed [25]. The present numerical code represents the most advanced unsteady, radiative, 1D flame modeling and it would be available for free download on our website.

4. Results and discussion

4.1. Validation of radiation model and radiation in spherical geometry

To validate the radiation model presented from Eq. (5) to Eq. (13) in a spherical geometry, we first compare the net radiation flux at the outside black boundary of a hollow sphere with inner and outer radii r_1 and r_2 (Fig. 1). The medium in the hollow sphere has a unity emissive power and no externally incident intensity at boundaries. For a given $r_2 - r_1$, the ratio of r_1/r_2 represents the curvature of the hollow sphere. The normalized radiation fluxes are plotted as a function of $r_2 - r_1$ for two different r_1/r_2 ratios and compared with the analytical solution [42]. It is seen that for both cases, the present numerical results agree extremely well with the theory. In addition, the results show that the increase of hollow sphere curvature at a given optical thickness has less radiation loss. This is obvious because the emitting gas volume becomes smaller at smaller r_1/r_2.

To validate the FSNB-CK model for spectral radiation, we calculated the volumetric radiation heat loss for water vapor (at 1000 K) in a hollow sphere. At $r_1/r_2 = 1$, the hollow sphere becomes a slab, so that the results can be compared with those in [33] in which the radiation heat loss was calculated from the SNB model using a ray tracing method. Figure 2 shows that the present FSNB-CK model can well reproduce the results in [33]. However, unlike the method in [33], the present method only requires computation time proportional to the grid number without loss of accuracy. Therefore, the present FSNB-CK model is accurate and computationally efficient. The volumetric heat loss for a solid sphere ($r_1 = 0$) is also shown in Fig. 2. It is seen that comparing to the slab radiation, the heat loss in the solid sphere case is much larger near the outside boundary.

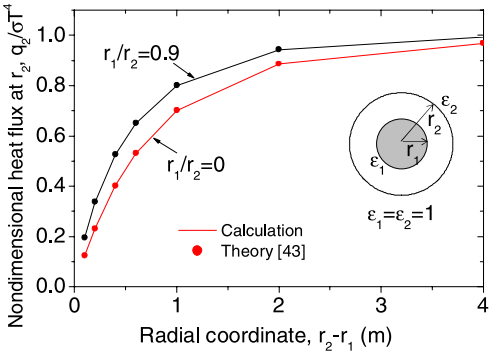

Fig. 1. Comparison of the predicted radiation flux at the outside hollow sphere boundary with theory for a gray emitting media with unity radiation power. Both boundaries are black.

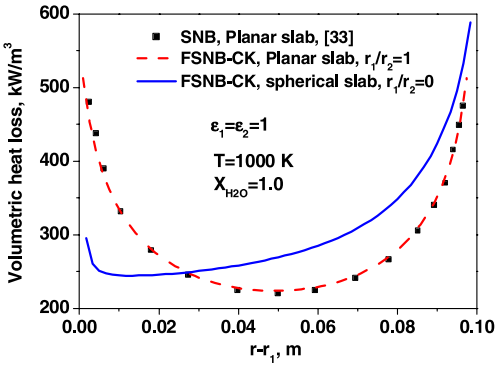

Fig. 2. Comparison of predicted volumetric heat loss for spectral dependent H_2O vapor radiation in a hollow sphere with a uniform temperature distribution and black boundaries.

However, the radiation heat loss at the center of the sphere becomes smaller. Therefore, the radiation geometry has a great impact on the local radiation heat loss. This will become clearer in the following flame speed comparisons.

4.2. Effect of radiation absorption on flame speed at elevated pressures

Figure 3a shows Schlieren photographs of $CH_4 - \{0.3O_2 + 0.2He + 0.5CO_2\}$ flames at different equivalence ratios at 1 atm. For fast-burning mixtures (stoichiometric or near stoichiometric mixtures, $\phi = 0.8$ in Fig. 3a), buoyancy effect is not observed from flame images and the flame front is spherically symmetric. For lean mixtures, the effect of buoyancy is noticeable and the flame front reaches the top edge of the photograph before reaching the bottom. Here, we define the 1-g downward flammability limit, Φ_d, as in the limiting mixture in which the flame can propagate throughout the whole chamber.For the present $CH_4 - \{0.3O_2 + 0.2He + 0.5CO_2\}$ mixture, the downward flammability limit is $\Phi_d = 0.50$. Below this limit, e.g. for leaner mixtures ($\phi = 0.49$ in Fig. 3a), the flame cannot propagate downward against buoyancy forces. After reaching the top of the inner chamber, the flame spreads out and propagates downward. Although the mixture at this condition is still flammable, the flame front location is hard to determine and flame speed data are not extracted for these cases. At elevated pressures, buoyancy effect is enhanced with the increase of mixture density. For example, at 5 atm the downward flammability limit becomes $\Phi_d = 0.57$.

Figure 3b shows measured and predicted flame speeds of $CH_4 - \{0.3O_2 + 0.2He + 0.5CO_2\}$ flames at different equivalence ratios at 1 atm. For comparisons, three radiation models were employed. First is the optically thin model (OPTM) in which no

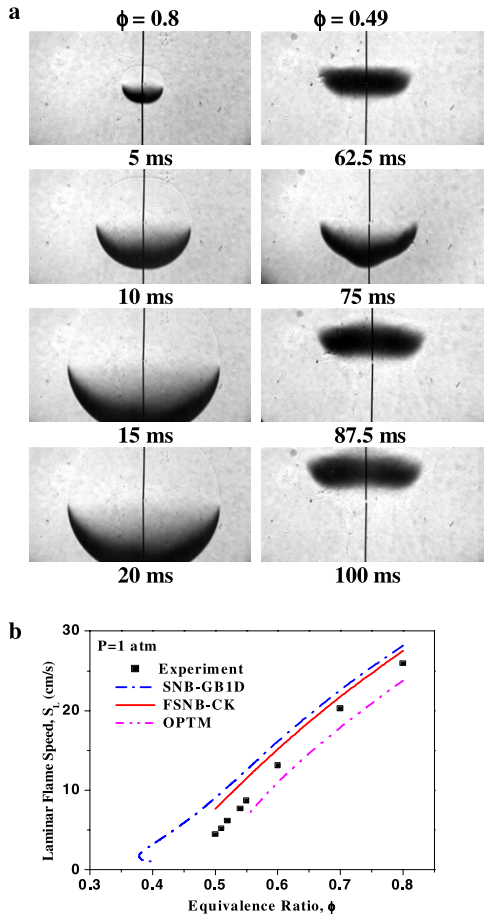

Fig. 3. (a) Schlieren photographs of $CH_4 - \{0.3O_2 + 0.2He + 0.5CO_2\}$ flames at different equivalence ratios at 1 atm; (b) measured and predicted laminar flame speeds of $CH_4 - \{0.3O_2 + 0.2He + 0.5CO_2\}$ flames as a function of equivalence ratio at 1 atm.

radiation absorption is considered. The second is the SNB gray band model in 1D planar geometry (SNB-GB1D) [21,33,42] in which gray gas model is used at each band (375 bands in total) and radiation absorption is solved in the one-dimensional slab rather than in spherical geometry. The third one is the present FSNB-CK model in which spectral radiation is solved in the spherical coordinate. Furthermore, the volumetric radiation heat losses and temperature distributions predicted from OPTM, SNB-GB1D and FSNB-CK for flames at equivalence ratio of 0.6 and flame radius of 2.4 cm are plotted in Fig. 4.

Figure 3b shows that the optically thin model under predict the flame speed. This is because OPTM model over predicts the radiation heat loss and the flame temperature decreases significantly in the burned zone (Fig. 4). However, for the

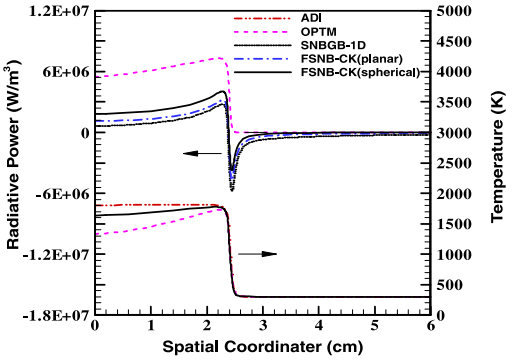

Fig. 4. Temperature and volumetric heat loss distributions in spherical $CH_4 - \{0.3O_2 + 0.2He + 0.5CO_2\}$ flame at $\Phi = 0.6$ and $P = 1$ atm.

FSNB-CK model, it is seen that because of radiation absorption, the radiation heat loss in the burned zone becomes much smaller. There is a significant amount of radiation heat loss that is reabsorbed by the unburned mixture (see the part with negative heat loss in Fig. 4) from the burned zone. This means that the radiation absorption in CO_2 diluted flames increases the flame speed by reducing the net heat loss and that the optically thin model is not applicable. As the equivalence ratio decreases, it is seen from Fig. 3b that radiation absorption plays an increasing role in increasing the flame speed and extending the flammability limit. On the other hand, the SNB gray band model in 1D geometry significantly over-predicts the flame speed. This over-prediction comes from two sources. One is that the employment of one-dimensional radiation geometry in which more radiation emission in the burned gas than that in the spherical flame was calculated (compare the radiation predicted by FSNB-CK(planar) and FSNB-CK(spherical) in Fig. 4); and the second is that the gray narrow band assumption increases the radiation absorption (compare the radiation predicted by FSNB-CK(planar) and SNB-GB1D in Fig. 4). The present FSNB-CK model greatly improved the flame speed prediction. A slight over-prediction may be resulted from the linear extrapolation method for flame speed because, strictly speaking, the radiation enhancement does not linearly increase with the flame radius. This improvement is because the radiation in spherical flame geometry is appropriately solved and the spectral radiation in each band is accurately treated by using the cumulative function of k-distribution from the direct Laplace transform instead of a simple gray assumption [4].

Theoretical analysis in [18] shows that radiation absorption has less effect as pressure increases because the total chemical heat release increases with the pressure. In order to examine the effect of pressure, the radiation absorption effect and comparison of different radiation model for $CH_4 + \{0.3O_2 + 0.2He + 0.5CO_2\}$ mixtures at 2 atm is shown in Fig. 5. It is seen that radiation absorption becomes much stronger than that at 1 atm. Different from the theory [18], the present result shows that radiation absorption increases with pressure. This is because an infinite optical thickness was assumed in the theory so that all the radiation heat loss from the burned zone will be absorbed by the unburned mixture. In the present experiment, the optical thickness is finite (about 1.0–6.0 estimated from OPTM) so that the increase of pressure enlarges the optical thickness and radiation absorption. Again, for the same reason, it is clearly seen that the present FSNB-CK model predicts the flame speed much better than SNB-GB1D. With a further increase of pressure, Fig. 6 shows that the radiation absorption effect further increases.

To further demonstrate the pressure effect on radiation absorption, the normalized flame speed increase due to radiation absorption at different equivalence ratio is plotted in Fig. 7. It is seen that the radiation absorption enhancement on flame speed is linearly dependent on pressure. This linear dependence is caused by the increase of optical

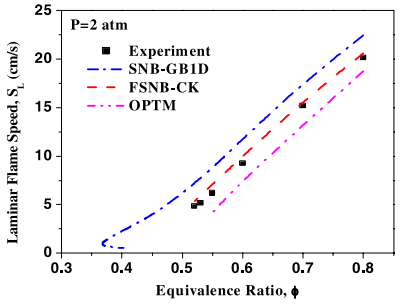

Fig. 5. Measured and predicted laminar flame speeds of $CH_4 - \{0.3O_2 + 0.2He + 0.5CO_2\}$ flames as a function of equivalence ratio at 2 atm.

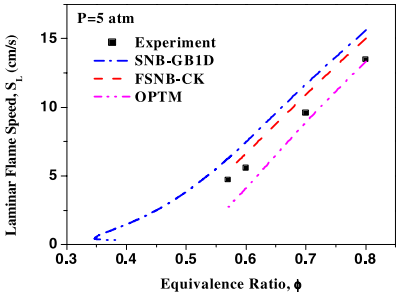

Fig. 6. Measured and predicted laminar flame speeds of $CH_4 - \{0.3O_2 + 0.2He + 0.5CO_2\}$ flames as a function of equivalence ratio at 5 atm.

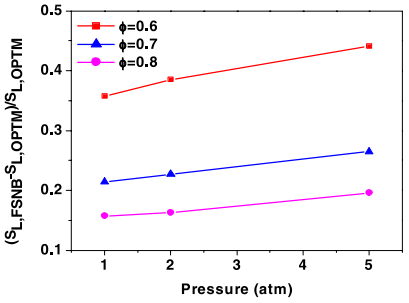

Fig. 7. Effects of radiation absorption on flame speed at different pressure and equivalence ratios.

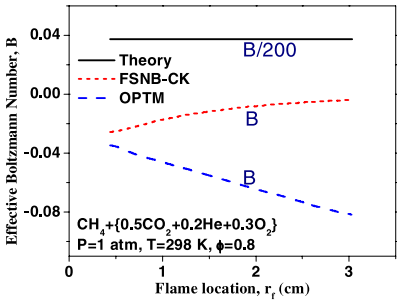

Fig. 8. The predicted effective Boltzmann number versus flame size at 1 atm.

thickness. In addition, Fig. 7 shows that with the decrease of equivalence ratio, the effect of radiation absorption on flame speed becomes more significant. Therefore, it can be concluded that although the pressure increase leads to an increased chemical heat release, the effect of radiation absorption on flame speed enhancement still increases and becomes increasingly important for lean flames.

As discussed above, the radiation absorption depends on the optical thickness. Therefore, it will be interesting to show how the radiation absorption enhancement on flame speed depends on flame size so that a flamelet model can be used to correct the radiation absorption effect in turbulence modeling. According to the theory [14], the flame speed is related with the Boltzmann number, B, by

$$(S_L/S_L^0)\ln(S_L/S_L^0) = B,$$
$$B = E\sigma(T_{ad}^4 - T_0^4)/(2R\rho_0 S_L^0 C_p T_{ad}^2) \quad (14)$$

where E, R, σ, and C_p denote the activation energy, universal gas constant, Stefan–Boltzmann constant, and the specific heat, respectively. T_{ad} is the adiabatic flame temperature, and ρ_0 and T_0 are the unburned gas density and temperature. Therefore, B represents the radiation absorption effect on the increase of flame speeds. The effective B numbers estimated from theory [18] and computation [by using S_L from simulation and the first equation of Eq. (14)] as a function of flame size are plotted in Fig. 8. Note that in calculating the B number, the flame stretch effect is already excluded by comparing the radiative flames with the adiabatic flames. It is seen that the radiation absorption effect predicted by the theory is two-order magnitude higher than that predicted by the FSNB-CK model. In addition, the theory predicts a constant B number with the increase of flame radius. This is also because of the assumption of large optical thickness. The FSNB-CK model predicts a negative B number at small flame radius and an increasing dependence of B on the flame radius. This means that at small flame radius, although radiation absorption can enhance the flame speed, the final flame speed remains below the adiabatic flame speed. However, with the increase of flame radius, the optical thickness increases, yielding an increase in B number. Again, for the optically thin model, the predicted B number is much lower. At high pressures, similar trends are also found except that the B number becomes positive at 2 atm. Therefore, by computing the B number for a given optical thickness, the radiation absorption effect can be employed in flamelet model for turbulent modeling.

5. Conclusions

The spectral dependent radiation absorption effect on flame speed enhancement was measured by using CO_2 diluted CH_4–O_2 mixtures at normal and elevated pressures. A new accurate FSNB-CK model was developed and validated for radiation computation of spherical propagating flames. The following conclusions were drawn from this study:

1. Radiation absorption increases the flame speed and extends the flammability limit. This enhancement effect also increases with pressure. The spectral dependent radiation absorption needs to be included in any quantitative predictions of flame speed and flammability limit with CO_2 addition.
2. The present radiation model can well reproduce the theoretical radiation flux at hollow sphere boundaries and the measured flame speed. The SNB narrow-band gray model over-predicts the flame speed while the optically thin model significantly under-predicts the flame speed.
3. The radiation absorption effect increases with flame size and pressure. The theory based on gray gas model over-predicts the radiation absorption by two-orders. The effective Boltzmann number is extracted from the present radiation modeling and can be applied to flamelet modeling in turbulent flow.

4. Flame geometry has a significant effect on flame radiation. In spherical flame modeling, the one-dimensional slab radiation model over-predicts the radiation absorption.

Acknowledgments

This work was partially supported by NASA Microgravity Research grant (NNC04GA59G) and DOE Project (DE-FG26-06NT42716).

References

[1] Y. Ju, T. Niioka, K. Maruta, *Appl. Mech. Rev.* 54 (2001) 257.
[2] C.K. Law, F.N. Egolfopoulos, *Proc. Combust. Inst.* 23 (1990) 413.
[3] M. Sibulkin, A. Frendi, *Combust. Flame* 82 (1990) 334.
[4] K.N. Lakshmisha, P.J. Paul, H.S. Mukunda, *Proc. Combust. Inst.* 23 (1990) 433.
[5] A. Abbud-Madrid, P.D. Ronney, *Proc. Combust. Inst.* 23 (1990) 423.
[6] J.A. Platt, J.S. T'ien, in: Fall Technical Meeting, Eastern Section of the Combustion Institute, 1990.
[7] K. Maruta, M. Yoshida, Y. Ju, T. Niioka, *Proc. Combust. Inst.* 26 (1996) 1283.
[8] C.J. Sung, C.K. Law, *Proc. Combust. Inst.* 26 (1996) 865.
[9] H. Guo, Y. Ju, K. Maruta, T. Niioka, F. Liu, *Combust. Flame* 109 (1997) 639.
[10] Y. Ju, H. Guo, K. Maruta, F. Liu, *J. Fluid Mech.* 342 (1997) 315.
[11] J. Buckmaster, *Combust. Theory Model.* 1 (1997) 1.
[12] Y. Ju, H. Guo, K. Maruta, T. Niioka, *Combust. Flame* 113 (1998) 113.
[13] Y. Ju, G. Masuya, F. Liu, H. Guo, K. Maruta, T. Niioka, *Proc. Combust. Inst.* 27 (1998) 2151.
[14] Y. Ju, C.K. Law, K. Maruta, T. Niioka, *Proc. Combust. Inst.* 28 (2000) 1891.
[15] D.B. Spalding, *Proc. R. Soc. (Lond.)* A240 (1957) 83.
[16] J. Buckmaster, *Combust. Flame* 26 (1976) 151.
[17] G. Joulin, P. Clavin, *Acta Astronaut.* 3 (1976) 223.
[18] G. Joulin, B. Deshaies, *Combust. Sci. Technol.* 47 (1986) 299.
[19] D. Lozinski, J. Buckmaster, P.D. Ronney, *Combust. Flame* 97 (1994) 301.
[20] Y. Ju, G. Masuya, P.D. Ronney, *Proc. Combust. Inst.* 27 (1998) 2619.
[21] H. Guo, Y. Ju, K. Maruta, T. Niioka, F. Liu, *Combust. Sci. Technol.* 135 (1998) 49.
[22] M.S. Wu, P.D. Ronney, Y. Ju, in: 38th Aerospace Sciences Meeting and Exhibit, AIAA 2000-0851, 2000.
[23] J. Ruan, H. Kobayashi, T. Niioka, Y. Ju, *Combust. Flame* 124 (2001) 225.
[24] A. Abbud-Madrid, P.D. Ronney, *AIAA J.* 31 (1993) 2179.
[25] X. Qin, Y. Ju, *Proc. Combust. Inst.* 30 (2005) 233.
[26] L.S. Rothman, C.P. Rinsland, A. Goldman, S.T. Massie, D.P. Edwards, J.M. Flaud, A. Perrin, C. Camy-Peyret, V. Dana, J.V. Mandin, J. Schroeder, A. McCann, R.R. Gamache, R.B. Wattson, K. Yoshino, K.V. Chance, K.W. Jucks, L.R. Brown, V. Nemtchinov, P. Varanasi, *J. Quant. Spect. Radiative Transfer* 60 (1998) 665.
[27] N. Jacquinet-Husson et al., *J. Quant. Spect. Radiative Transfer* 62 (1999) 205.
[28] A. Soufiani, J. Taine, *Intl. J. Heat Mass Transfer* 40 (1997) 987.
[29] W.L. Grosshandler, *Radical, Int. J. Heat Mass Transfer* 23 (1980) 1147.
[30] M.K. Denison, B.W. Webb, *J. Heat Transfer* 117 (1995) 359.
[31] M.F. Modest, H. Zhang, *J. Heat Transfer* 124 (2002) 30.
[32] M.F. Modest, S.P. Bharadwaj, in: Proceedings of the ICHMT, 3rd International Symposium On Radiative Transfer, Antalya, Turkey, 2001.
[33] T.K. Kim, J.A. Menart, H.S. Lee, *J. Heat Transfer* 113 (1991) 946.
[34] H. Bedir, J.S. Tien, H.S. Lee, *Combust. Theory Model.* 1 (1997) 395.
[35] A.A. Lacis, V.A. Oinas, *J. Geophys. Res.* 96 (1991) 9027.
[36] F. Liu, G.J. Smallwood, Ö.L. Gülder, *J. Quant. Spect. Radiative Transfer* 68 (2001) 401.
[37] W.A. Fiveland, *J. Heat Transfer* 106 (1984) 699.
[38] D.B. Ludwig, W. Malkmus, J.E. Reardon, J.A.L. Thomson, NASA SP3080, 1973.
[39] E.F. Toro, M. Spruce, W. Speares, *Shock Waves* 4 (1994) 25.
[40] R.J. Kee, J.F. Grcar, M.D. Smooke, J.A. Miller, Sandia Report, SAND85-8240, Sandia National Laboratories, 1985.
[41] Available at http://www.me.berkeley.edu/gri_mech/.
[42] H. Greenspan, C.N. Kelber, D. Okrent (Eds.), *Comput. Methods Reactor Phys.*, Gordon and Breach, New York, 1968.

Comment

Derek Bradley, Leeds University, UK Can your analysis be applied to the conditions of very large flame radii, such as might occur in atmospheric explosions?

Reply. Yes. Since the optical thickness increases with flame radius, for the conditions of very large flame radii, the radiation emission and re-absorption become even more important. Therefore, the spectrally dependent radiation absorption effect on flame speed enhancement must be considered.